

Impact of T_e/T_i in H-mode confinement database

E. Narita¹, T. Takizuka², M. Iida¹, Y. Tanaka¹, A. Isayama², K. Itami², T. Fukuda¹

¹*Osaka University, Suita, Osaka 565-0871, Japan*

²*Japan Atomic Energy Agency, Naka, Ibaraki 311-0193, Japan*

Abstract

In order to improve the prediction capability of confinement time for burning plasmas, we examined the updated DB3v10 database with emphasis on the temperature ratio T_e/T_i , including consideration of kinetic profiles. The impact of T_e/T_i is more apparent with peaked density profiles cases than with flat density profiles cases. The confinement scaling with contribution of T_e/T_i was elaborated. In this process, the contributions of kinetic profiles to confinement are observed. However, inherent the role of turbulence, such as ITG and TEM might affect the contribution of kinetic profiles.

1. INTRODUCTION

Scaling expressions for thermal energy confinement time have very important role in predicting the future devices. Among them, the most well-known scaling expression is IPB98(y,2)^[1], which was elaborated from the international H- mode confinement database consists of dominantly ion-heated discharges. However, in a burning machine, like ITER, intensive electron heating is anticipated^[2]. Hence the utmost objective of this work is to improve the prediction capability for confinement properties in burning plasmas with emphasis on the contribution of T_{e0}/T_{i0} , incorporating 2D-profile information^[3]. Moreover, we aim to establish semi-2D confinement scaling with considerations of kinetic profiles, and to identify the inherent turbulence.

2. SIGNIFICANCE OF T_e/T_i AND PROFILE SHAPES

We extracted the 67 data from ASDEX Upgrade (AUG), 68 data from Alcator C-Mod (C-Mod), and 16 data from DIII-D with $0.60 < I_p[\text{MA}] < 1.93$, $0.94 < B_t[\text{T}] < 5.82$, $2.86 < n_e[10^{19} \text{m}^{-3}] < 42.6$, $3.05 < q_{95} < 8.31$, $1.42 < \kappa_a < 1.81$, and $0.11 < \delta < 0.696$. Here, I_p , B_t , n_e , q_{95} , κ_a and δ are plasma current, toroidal magnetic field, electron density, plasma safety factor at 95% flux surface, triangularity, and ellipticity, respectively. The density is lower than 60% of

the Greenwald density limit $n_{\text{GW}} \equiv I_p/\pi a^2$ in order to avoid concerns other than transport. Firstly, we divided data into two into two groups, $1.0 < n_{e0}/n_{eL} < 1.1$ and $1.1 < n_{e0}/n_{eL} \leq 1.2$, in first group, the electron density profiles are flat, and in second group, the profiles are peaked. Then according to range of n_{e0}/n_{eL} , we elaborated confinement scaling with ‘engineering’ variables which are used in IPB98(y,2).

$$\tau_{\text{sc},a} = 0.0777 I_p^{0.91} B_t^{0.11} n_e^{0.28} P_L^{-0.59} R^{1.73} M^{0.27} \varepsilon^{0.54} \kappa_a^{0.41} : 1.0 < n_{e0}/n_{eL} < 1.1 \quad (1)$$

$$\tau_{\text{sc},b} = 0.0594 I_p^{0.90} B_t^{0.08} n_e^{0.34} P_L^{-0.63} R^{1.78} M^{0.16} \varepsilon^{0.41} \kappa_a^{0.72} : 1.1 < n_{e0}/n_{eL} < 1.6 \quad (2)$$

The ‘engineering’ variables are I_p [MA], B_t [T], n_e [10^{19} m^{-3}], P_L = loss power[MW], R [m] = major radius[m], M = ion mass, ε = inverse aspect ratio, and κ . These scaling expressions are similar, except density dependence is slightly enhanced in case peaked n_e . Figure 1 shows the relation between the H-factor and the temperature ratio. H-factor is ratio between experimental confinement time τ_{th} and τ_{sc} , and we defined that $H_{\text{Ha}} = \tau_{\text{th}}/\tau_{\text{sc},a}$ and $H_{\text{Hb}} = \tau_{\text{th}}/\tau_{\text{sc},b}$. In flat $n_e(r)$, the impact of T_{e0}/T_{i0} was obscure. On the other hand, in peaked $n_e(r)$, the impact seems more pronounced in comparison with the case flat $n_e(r)$. Next, we divided peaked $n_e(r)$ data into (I) $T_{e0}/T_{i0} < 1$ and (II) $T_{e0}/T_{i0} > 1$, and the contributions of kinetic profiles are investigated in (I) and (II) range. Here n_e profile n_{e0}/n_{eL} and internal inductance l_i are chosen as kinetic profiles. Figure 2(a) and (b) are dependence of H-factor on n_{e0}/n_{eL} in (I) and (b), respectively. In range (I), confinement improves with peaked n_{e0} , meanwhile, in range (II), peaked n_{e0} slightly deteriorate confinement. Second, the dependence of H-factor normalized by n_{e0}/n_{eL} on l_i is investigated in order to eliminate the n_{e0}/n_{eL} dependence. In range (I), the increase in l_i also improve confinement (Fig.3 (a)), on the other hand, in range (II), contribution of l_i is subtle (Fig.3 (b)).

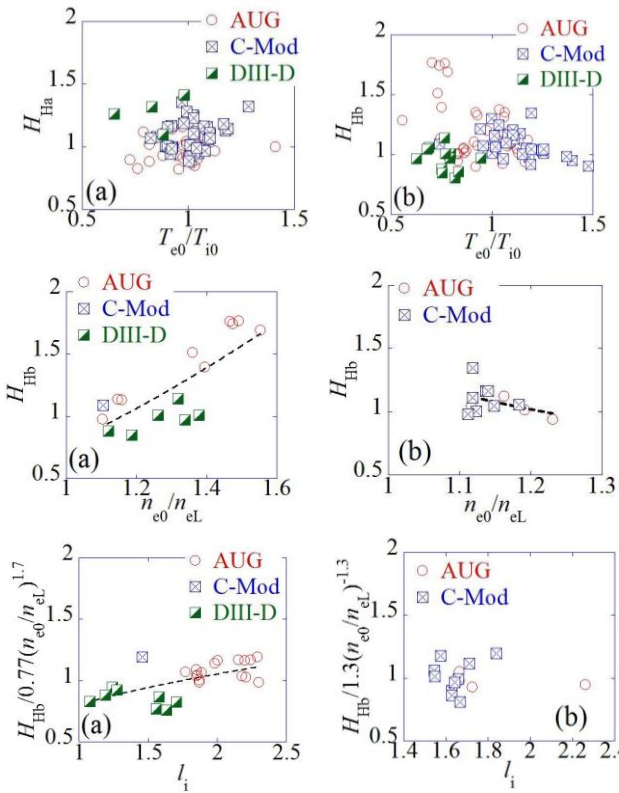


Figure 1. Distribution of T_{e0}/T_{i0} to (a) H_{Ha} , and to (b) H_{Hb}

Figure 2. Distribution of n_{e0}/n_{eL} to H_{Hb} (a) In $T_{e0}/T_{i0} < 1$, range $0.70 < T_{e0}/T_{i0} < 0.80$ is extracted. H_{Hb} is almost proportional to $(n_{e0}/n_{eL})^{1.7}$ (b) In $T_{e0}/T_{i0} > 1$, range $1.07 < T_{e0}/T_{i0} < 1.20$ is extracted. H_{Hb} is almost proportional to $(n_{e0}/n_{eL})^{-1.3}$

Figure 3. Distribution of l_i to H_{Hb} normalized n_{e0}/n_{eL} (a) In $T_{e0}/T_{i0} < 1$, range $0.70 < T_{e0}/T_{i0} < 0.90$ is extracted. H_{Hb} is almost proportional to $l_i^{0.39}$ (b) In $T_{e0}/T_{i0} > 1$, range $1.10 < T_{e0}/T_{i0} < 1.20$ is extracted. Dependence on l_i is subtle.

3. INDICATION OF UNDERLYING TURBULENCE

In this section, we observed the contribution of T_{e0}/T_{i0} to H-factor from which the dependences on n_{e0}/n_{eL} and l_i are eliminated (figure 4). In both range, The confinement deteriorates T_{e0}/T_{i0} as moves away from 1, but this is against that the fundamental role of T_{e0}/T_{i0} is positive in $T_{e0}/T_{i0} < 1$, so this might mean that underlying turbulence, such as ITG and TEM, might be influencing confinement in both $T_e/T_i < 1$ and $T_e/T_i > 1$ regimes.

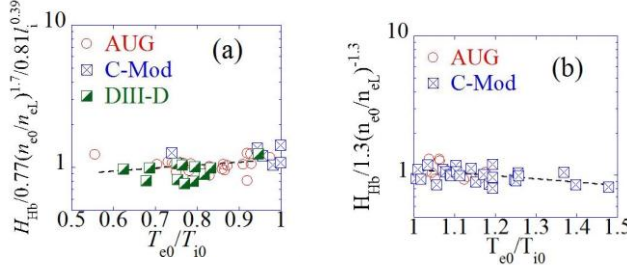


Figure 4. Distribution of T_e/T_i to H_{Hb} normalized n_{e0}/n_{eL} and l_i . (a) $T_{e0}/T_{i0} < 1$, (b) $T_{e0}/T_{i0} > 1$

4. SCALING INCLUDING T_e/T_i

In the previous section, we have not observed the role of ITG and TEM clearly. Hence we emphasized on figure 1(a) again. In case that we consider the points from AUG and C-Mod which have broad range of T_e/T_i , the increase in T_e/T_i deteriorate confinement in both $T_e/T_i < 1$ and $T_e/T_i > 1$. Then we elaborate confinement scaling without dividing data based on T_e/T_i with 3 nondimensional valuables ^[4], namely $B_t R^{1.25}$, n/n_{GW}^* and q are used. $(n/n_{GW}^*) = n_e / (n_{GW} \times (a/0.5)^{0.25})$, $q = (1 + \kappa_a^2) B_t a^2 / (R I_p)$. Improvement rate is defined as $(H_{Hb} - 1) / (T_{e0}/T_{i0} - 1)$, and we assumed that the improvement rate is expressed as $(H_{Hb} - 1) / (T_{e0}/T_{i0} - 1) = C \times (B_t R^{1.25})^\alpha \times (n/n_{GW}^*)^\beta \times q^\gamma$. Moreover we added the data from JET to expand the ranges of 3 nondimensional valuables. In order to find α , β and γ , the data is divided into $(H_{Hb} - 1) / (T_{e0}/T_{i0} - 1) < 0$ and $(H_{Hb} - 1) / (T_{e0}/T_{i0} - 1) > 0$ range, and in each range, following confinement scaling were obtained.

$$\tau_{sc,c} = \tau_{sc,b} \times \{1 - 0.157 \times (T_{e0}/T_{i0} - 1) \times (B_t R^{1.25})^{0.59}\} : (H_{Hb} - 1) / (T_{e0}/T_{i0} - 1) < 0 \quad (3)$$

$$\tau_{sc,d} = \tau_{sc,b} \times \{1 + 0.913 \times (T_{e0}/T_{i0} - 1) \times (B_t R^{1.25})^{-0.81}\} : (H_{Hb} - 1) / (T_{e0}/T_{i0} - 1) > 0 \quad (4)$$

When this confinement scaling was applied in the dataset from AUG, C-Mod, DIII-D, JET and JT-60U, the standard deviation σ ($\sigma^2 = N^{-1} \sum (\tau_{th} / \tau_{sc,c,d} - 1)^2$) is 1.47, while in case that $\tau_{sc,b}$ not including T_{e0}/T_{i0} is used, $\sigma = 0.183$. In addition, when we have assumption that condition $T_{e0}/T_{i0} > 1$ leads $H_{Hb} < 1$ in burning plasmas, the correcting term $f = 0.157 \times (T_{e0}/T_{i0} - 1) \times (B_t R^{1.25})^{0.59}$ in (3) was plotted against n_{e0}/n_{eL} (Fig.5). It was documented that peaked density profiles contribute to an improvement of confinement for $T_{e0}/T_{i0} < 1$ range, and degradation for $T_{e0}/T_{i0} > 1$ range. The results in this section agree well with ones in the section 2.

The confinement scaling $\tau_{sc,c,d}$ improves prediction capability on in terms of the distribution of plots from JET data. Fig.6 (a) shows $\tau_{sc,b}$ versus τ_{th} , and Fig.6 (b) shows $\tau_{sc,c,d}$

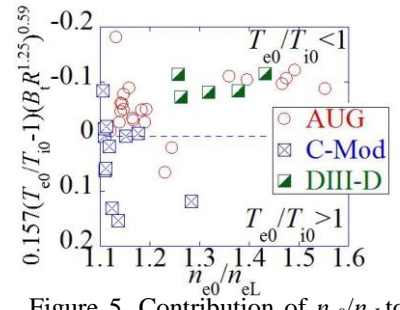


Figure 5. Contribution of n_{e0}/n_{eL} to the correcting term in (3)

versus τ_{th} . We introduce $\Delta\tau_{\text{sc,b}} = \tau_{\text{th}} - \tau_{\text{sc,b}}$ and $\Delta\tau_{\text{sc,c,d}} = \tau_{\text{th}} - \tau_{\text{sc,c,d}}$, and observe the variation of $\Delta\tau_{\text{sc,b}}$ and $\Delta\tau_{\text{sc,c,d}}$ against τ_{th} . We chose the representative points at values of $\tau_{\text{th}} = 0.2, 0.3 \dots 0.8$, and the averages of each value are defined as $\Delta\tau_{\text{sc,b,ave}}$ and $\Delta\tau_{\text{sc,c,d,ave}}$. In Fig.7, $\Delta\tau_{\text{sc,b,ave}}$ and $\Delta\tau_{\text{sc,c,d,ave}}$ are plotted against τ_{th} . In data using $\tau_{\text{sc,b}}$, the variation of $\Delta\tau_{\text{sc,b,ave}}$ against τ_{th} is wider than in data using $\tau_{\text{sc,c,d}}$. This describes that the distribution of plots from JET data is straighter in case $\tau_{\text{sc,c,d}}$ is used.

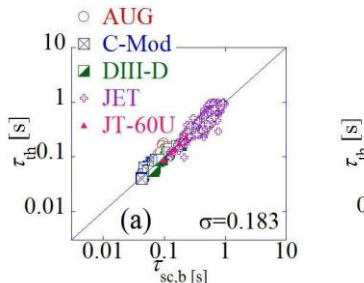


Figure 6. Comparison of experimental confinement time τ_{th} with (a) $\tau_{\text{sc,b}}$, and (b) $\tau_{\text{sc,c,d}}$ including T_e/T_i

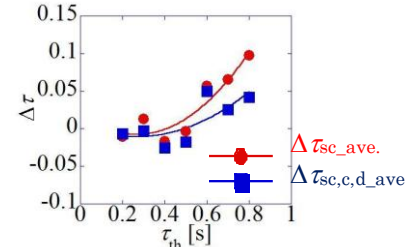
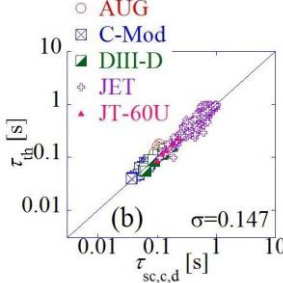


Figure 7.
 $\Delta\tau$ dependence on τ_{th}

5. CONCLUSION

In our work, the impact of T_e/T_i have been examined, consideration of kinetic profiles. As a consequence, noticeable contribution of T_e/T_i was observed. In particular, impact of T_e/T_i seems more pronounced for discharges with peaked density profiles. Kinetic profiles has differences in contribution to confinement, in $T_{e0}/T_{i0} < 1$ region both n_{e0}/n_{eL} and l_i improve confinement, while in $T_{e0}/T_{i0} > 1$ region increase in n_{e0}/n_{eL} slightly deteriorate confinement, and contribution of l_i is subtle. The roles of ITG in $T_e/T_i < 1$, TEM in $T_e/T_i > 1$ are also indicated.

6. DISCUSSION

In this work, we have found the tendency of improvement of prediction capability with consideration of T_e/T_i . The contributions of kinetic profiles, however, were not included in the confinement scaling, because underlying turbulence, such as ITG and TEM, might be influence the dependences on n_{e0}/n_{eL} and l_i . In order to predict confinement time, the better understanding of the dependences on inherent turbulence is required. The GS2 analysis is under progress to identify the related dynamics in turbulence.

References

- [1] ITER Physics Expert Groups on Confinement and Transport and Confinement Modelling and Database, Nucl. Fusion 39, 2175 (1999).
- [2] T. H. Stix, Plasma Phys. 14, 367 (1972).
- [3] O. Kardaun et al., Fusion Energy 2000 (2000) ITERP/04.
- [4] T Takizuka JAERI-Research 95-075 (1995).
- [5] J Weiland, Plasma phys. Contro. Fusion 47 (2005) 441-449